

the physiological event underlying the macroscopic signs of oxidative metabolism, all of which occur within the first seconds after onset of induced activity. The spatial confinement of the NADH dip to dendrites further supports our view, since the preferred localization of cytochrome oxidase is in postsynaptic dendritic areas (28).

The kinetics of the late astrocyte NADH response as an indicator of enhanced glycolysis are in accord with reports that demonstrated nonoxidative glucose consumption during induced brain activity (1, 29). Note that the temporal resolution of PET or NMR spectroscopy would not have permitted the detection of early oxidative metabolism in these studies. However, one study (30) using a microsensor with significantly higher temporal resolution described a biphasic change in extracellular lactate with an early decrease (duration 10 to 12 s), followed by a long-lasting overshoot (peak after ~60 s). This result is in full agreement with our model, which is based on our ample resolution in both space and time.

Our results confirm that early neuronal oxidative metabolism is the default response to increased neural activity. Only after a significant period (~10 s) with depletion of substrates for oxidative metabolism (9, 30) is astrocytic glycolysis activated. Thereby, extracellular lactate might serve as a buffer preventing activation of the astrocyte-neuron lactate shuttle during minor or short-lasting neural activity. The observation that the transient NADH production as an indicator of nonoxidative glycolysis in astrocytes exceeds neuronal NADH consumption and further increases with longer stimulation strengthens this interpretation.

Our model integrates existing views of the organization of brain energy metabolism during focal neural activity (1–3, 5) and has direct implications for the design and interpretation of functional neuroimaging studies: The discovery that early oxidative metabolism is entirely neuronal strengthens the motivation for the current search for the initial dip in BOLD-fMRI, and the confinement of glycolysis to astrocytes implies that ¹⁸F-fluorodeoxyglucose-PET studies measure glucose uptake into the glial and not the neuronal compartment during focal neural activity.

References and Notes

- P. T. Fox, M. E. Raichle, M. A. Mintun, C. Dence, *Science* **241**, 462 (1988).
- D. Malonek, A. Grinvald, *Science* **272**, 551 (1996).
- F. Hyder et al., *Proc. Natl. Acad. Sci. U.S.A.* **93**, 7612 (1996).
- L. Pellerin, P. J. Magistretti, *Proc. Natl. Acad. Sci. U.S.A.* **91**, 10625 (1994).
- N. R. Sibson et al., *Proc. Natl. Acad. Sci. U.S.A.* **95**, 316 (1998).
- A. Schurr, J. J. Miller, R. S. Payne, B. M. Rigor, *J. Neurosci.* **19**, 34 (1999).
- B. Voutsinos-Porche et al., *Neuron* **37**, 275 (2003).

- C. P. Chih, P. Lipton, E. L. Roberts Jr., *Trends Neurosci.* **24**, 573 (2001).
- S. Mangia et al., *Neuroscience* **118**, 7 (2003).
- D. L. Rothman et al., *Philos. Trans. R. Soc. London Ser. B* **354**, 1165 (1999).
- W. Denk, J. H. Strickler, W. W. Webb, *Science* **248**, 73 (1990).
- B. D. Bennett, T. L. Jetton, G. Ying, M. A. Magnuson, D. W. Piston, *J. Biol. Chem.* **271**, 3647 (1996).
- G. H. Patterson, S. M. Knobel, P. Arkhammar, O. Thastrup, D. W. Piston, *Proc. Natl. Acad. Sci. U.S.A.* **97**, 5203 (2000).
- B. Chance, G. R. Williams, *J. Biol. Chem.* **217**, 409 (1955).
- X. Aubert, B. Chance, R. D. Keynes, *Philos. Trans. R. Soc. London Ser. B* **160**, 211 (1964).
- J. R. Williamson, B. E. Herzig, H. S. Coles, W. Y. Cheung, *J. Biol. Chem.* **242**, 5119 (1967).
- B. Chance, H. Baltscheffsky, *J. Biol. Chem.* **233**, 736 (1958).
- L. K. Klaidman, A. C. Leung, J. D. J. Adams, *Anal. Biochem.* **228**, 312 (1995).
- D. K. Merrill, R. W. Guynn, *J. Neurochem.* **27**, 459 (1976).
- D. K. Merrill, R. W. Guynn, *Brain Res.* **221**, 307 (1981).
- P. Lipton, *Biochem. J.* **136**, 999 (1973).
- C. W. Shuttleworth, A. M. Brennan, J. A. Connor, *J. Neurosci.* **23**, 3196 (2003).
- F. F. Jobsis, M. O'Connor, A. Vitale, H. Vreman, *J. Neurophys.* **34**, 735 (1971).
- R. Brandes, D. M. Bers, *Biophys. J.* **71**, 1024 (1996).
- L. Pellerin, P. J. Magistretti, *J. Cereb. Blood Flow Metab.* **23**, 1282 (2003).
- U. Lindauer et al., *Neuroimage* **13**, 988 (2001).
- J. K. Thompson, M. R. Peterson, R. D. Freeman, *Science* **299**, 1070 (2003).
- M. T. Wong-Riley, *Trends Neurosci.* **12**, 94 (1989).
- J. Prichard et al., *Proc. Natl. Acad. Sci. U.S.A.* **88**, 5829 (1991).
- Y. B. Hu, G. S. Wilson, *J. Neurochem.* **69**, 1484 (1997).
- We thank R. S. Balaban, L. Pellerin, and D. Piston for discussions and I. Tullis and A. Heikal for technical advice. K.A.K. thanks R. Love, F. Bergmann, S. Hess, B. T. Hyman, and A. C. Ludolph for support. Dedicated to Keiko Tsuno-Kasichke (†20 October 2003). This research was conducted in the Developmental Resource for Biophysical Imaging Opto Electronics, a NIH-NIBIB resource. Supported by the Deutsche Forschungsgemeinschaft (KA1490/2-1 and 2-2) and the National Institutes of Health (P41-EB001976-16).

Supporting Online Material

www.sciencemag.org/cgi/content/full/305/5680/99/DC1
Materials and Methods

SOM Text

Fig. S1

References

5 February 2004; accepted 21 May 2004

Inhibition of Netrin-Mediated Axon Attraction by a Receptor Protein Tyrosine Phosphatase

Chieh Chang,^{1,2} Timothy W. Yu,² Cornelia I. Bargmann,^{2,*}
Marc Tessier-Lavigne^{1*†}

During axon guidance, the ventral guidance of the *Caenorhabditis elegans* anterior ventral microtubule axon is controlled by two cues, the UNC-6/netrin attractant recognized by the UNC-40/DCC receptor and the SLT-1/slit repellent recognized by the SAX-3/robo receptor. We show here that loss-of-function mutations in *clr-1* enhance netrin-dependent attraction, suppressing ventral guidance defects in *slt-1* mutants. *clr-1* encodes a transmembrane receptor protein tyrosine phosphatase (RPTP) that functions in AVM to inhibit signaling through the DCC family receptor UNC-40 and its effector, UNC-34/enabled. The known effects of other RPTPs in axon guidance could result from modulation of guidance receptors like UNC-40/DCC.

Axons in the developing nervous system respond to attractive and repulsive guidance cues of the netrin, slit, semaphorin, and ephrin families (1–3). The interpretation of a guidance signal as a repellent or an attractant is context-dependent and influenced by the activities of other signaling pathways (4, 5). Thus, the netrin receptor UNC-40 contributes to both axon attraction (acting on its own) and repulsion (in coop-

eration with the second netrin receptor, UNC-5, or the slit receptor robo) (6–10).

Receptor protein tyrosine phosphatases (RPTPs) are implicated in axon growth and guidance (11, 12). In general, the inputs that regulate RPTPs, as well as their potential targets, are unknown. Phosphatases are presumed to affect axon guidance by antagonizing kinases, and many tyrosine kinases have been implicated in axon outgrowth and guidance (13–19).

The molecules that guide AVM axons toward the ventral midline in *C. elegans* are similar to those that direct commissural neurons toward the floor plate in vertebrate spinal cords. The AVM neuron sends its axon ventrally toward the attractant UNC-6/netrin (Fig. 1, A and B) and away from the dorsal repellent SLT-1. Mutations in either of these signaling systems result in a 30 to 40% penetrant defect in AVM ventral guidance,

¹Department of Biological Sciences, Howard Hughes Medical Institute (HHMI), Stanford University, Stanford, CA 94305, USA. ²Department of Anatomy and Department of Biochemistry and Biophysics, HHMI, University of California San Francisco (UCSF), San Francisco, CA 94143, USA.

*To whom correspondence should be addressed. E-mail: cori@itsa.ucsf.edu (C.I.B.); march@gene.com (M.T.L.)

†Present address: Genentech, Incorporated, 1 DNA Way, South San Francisco, CA 94080, USA.

REPORTS

whereas mutations in both systems together result in a near-complete failure of ventral guidance (20). Because there are two sources of guidance information, mutants that potentiate signaling through one guidance pathway might suppress the effects caused by loss of the other pathway. A *slt-1* (*null*) strain is therefore a useful genetic background to search for mutations allowing enhanced signaling through the *unc-6–unc-40* pathway.

We undertook two parallel approaches to the suppressor screen. First, we generated double mutants between *slt-1* and 30 genes implicated in axon guidance or cell migration and examined the resulting AVM phenotypes. Second, we clonally screened a mutagenized *slt-1* null mutant (~1000 genomes), selecting mutants that decreased the penetrance of its AVM guidance defect. Both approaches identified a single strong suppressor, in each case a mutation in the *clr-1* gene. The temperature-sensitive mutation *clr-1*(*e1745*), tested in the candidate screen, resulted in an almost-complete suppression of the AVM ventral guidance defect of *slt-1* null mutants (Fig. 1, C to E). A single mutation from the genetic screen, *cy14*, yielded a similar suppression of the ventral guidance defect and mapped to chromosome II near the

clr-1 locus. Complementation tests showed that *cy14* fails to complement the *clr-1*(*e1745*) mutant phenotype.

Sequencing the *clr-1* open reading frame in the *cy14* mutant revealed a molecular lesion for *cy14* (21), confirming that *cy14* represents a previously unknown *clr-1* allele. *cy14* is a G-to-A transition in the splice acceptor of intron 5 of *clr-1* that leads to the use of a cryptic splice acceptor and consequently to an 18-base-pair deletion in exon 6 (fig. S1, A and B). The mutant allele lacks part of the single immunoglobulin (Ig) domain in the extracellular region of CLR-1 (fig. S1C). CLR-1 encodes a transmembrane protein tyrosine phosphatase that antagonizes fibroblast growth factor receptor (FGFR) signaling (22). An alignment of vertebrate RPTP and CLR-1 catalytic domains assigns CLR-1 to the R5 subdivision of RPTP family members (23) (fig. S1D). However, the extracellular region of CLR-1 is more like the leukocyte common antigen-related protein subfamily of vertebrate RPTPs, because it contains an Ig domain and FN III (fibronectin type III) repeats (fig. S1D). These sequence features indicate that CLR-1 can be classified as an RPTP but not as the clear ortholog of a particular vertebrate RPTP.

Several models could explain the suppression of the *slt-1* mutant phenotype by the *clr-1* mutation. To distinguish between various possibilities, we examined the effects of the *clr-1* mutation in mutant backgrounds that disable elements of different guidance pathways. The *clr-1* null phenotype is lethal, and *clr-1*(*cy14*) is subviable, so these genetic studies were performed with the use of the temperature-sensitive *clr-1* allele *e1745ts*.

The *clr-1* mutation suppressed the AVM defects of a *sax-3* mutant (Fig. 1C), arguing that *clr-1* function is *sax-3*-independent. By contrast, the *clr-1* mutation failed to significantly suppress AVM defects of *unc-6*, *unc-40*, *unc-6 slt-1*, or *unc-40 slt-1* mutants (Fig. 1, C, F, and G). Because AVM guidance defects in *unc-6*, *unc-40*, *slt-1*, or *sax-3* mutants are comparable in severity, suppression of *slt-1* and *sax-3* appears to be pathway-specific. These results suggest that CLR-1 requires UNC-6 and UNC-40 to affect ventral guidance, consistent with the model that CLR-1 acts on UNC-6/UNC-40 signaling.

One way in which CLR-1 could antagonize netrin signaling would be to limit the production or distribution of UNC-6/netrin. To address this possibility, we examined an alternative response to UNC-6. The DA/DB

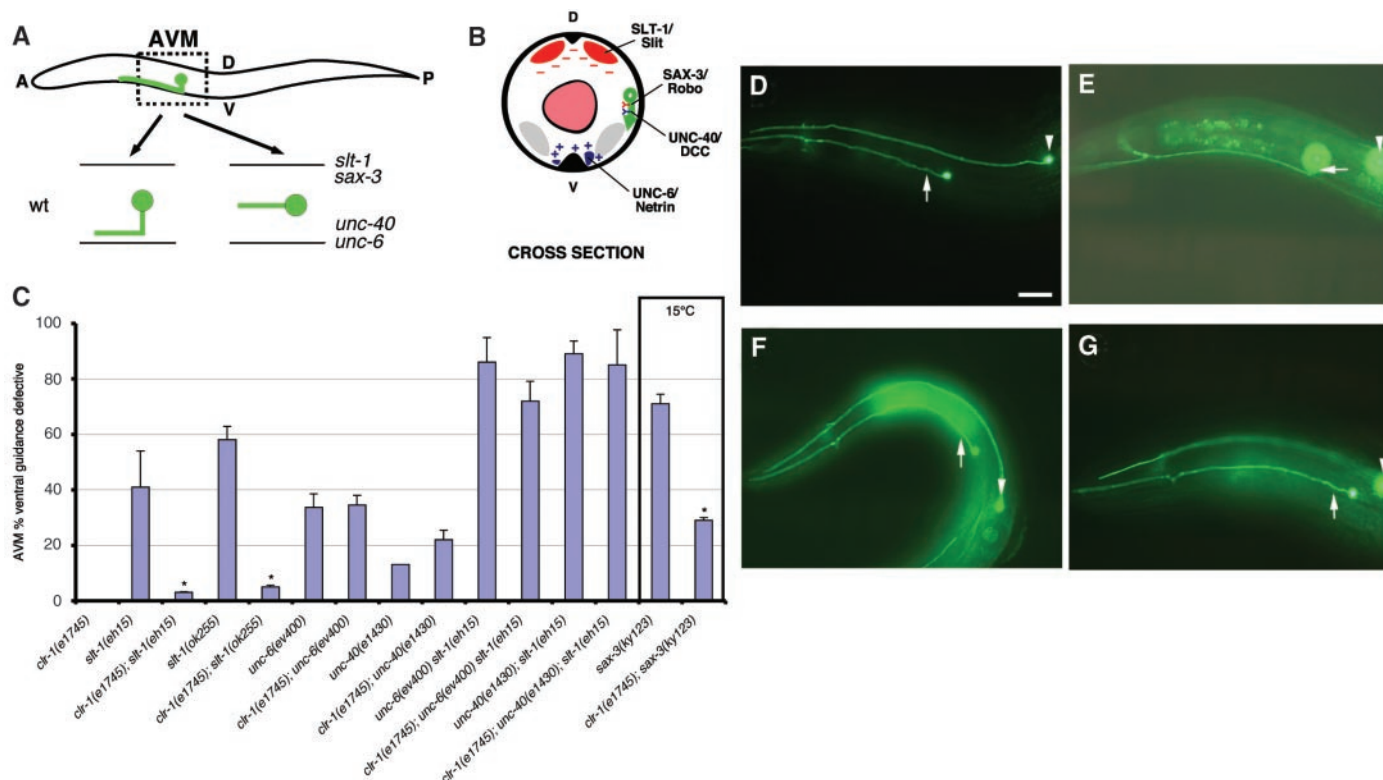


Fig. 1. *clr-1* regulates *unc-6/unc-40*-dependent guidance. (A) Schematic diagram of wild-type and mutant AVM axons. D indicates dorsal; V, ventral; A, anterior; P, posterior. (B) SAX-3/Robo and UNC-40/DCC guidance receptors in AVM (green) guide axons toward ventral UNC-6/netrin (blue) and away from dorsal SLT-1/slit (red). (C) *clr-1* mutation suppresses AVM guidance defects of *slt-1* and *sax-3* mutations but not *unc-6* and *unc-40* mutations. Because *clr-1* is essential for viability, we used a

temperature-sensitive partial loss-of-function *clr-1* allele, *e1745ts*. All other mutations were strong loss-of-function alleles. Strains were grown at 20°C except the *sax-3* and the *clr-1*; *sax-3* mutants. Asterisks indicate data significantly different from *clr-1*(+) controls ($P < 0.001$). AVM axon trajectories (arrow) labeled by *zdis5[mec-4::gfp]* in (D) *slt-1*, (E) *clr-1*; *slt-1*, (F) *unc-6*, and (G) *clr-1*; *unc-6*. Arrowhead, ALM cell body. Anterior is to the left; dorsal, up. Scale bar, 20 μ m.

motor axons use UNC-6 as a guidance cue, but they are repelled rather than attracted by ventral UNC-6 (Fig. 2A). Repulsion of DA/DB axons uses both UNC-40 and UNC-5 guidance receptors (24). *unc-5* mutants have a severe defect in DA/DB dorsal guidance, whereas *unc-40* defects in DA/DB guidance are milder (Fig. 2B). If CLR-1 normally acts to decrease netrin availability, a *clr-1* mutation might sup-

press the mild dorsal guidance defects of an *unc-40* mutant by making more UNC-6/netrin available for detection by UNC-5. Contrary to this prediction, the *clr-1* mutation resulted in a significant enhancement of *unc-40* mutant phenotypes in DA and DB axons (Fig. 2, B to D). This finding suggests a positive role for CLR-1 in netrin repulsion, in contrast with its inhibitory role in netrin attraction. CLR-1 also pro-

motes UNC-6–dependent dorsal mesodermal cell migrations (25). These genetic results argue against a common effect of CLR-1 on the netrin ligand. By implication, they suggest that, in AVM ventral guidance, CLR-1 normally limits the activity of the UNC-40 receptor.

CLR-1 could inhibit UNC-40 by acting either nonautonomously, for example as a transmembrane ligand for UNC-40, or autonomously in the netrin-responsive cell. A *clr-1::gfp* fusion gene is expressed in many cells whose normal guidance requires *unc-40*, including AVM, HSN, DD, VD, and mesodermal cells, suggesting an autonomous role (fig. S2). To ask where CLR-1 acts to regulate AVM attraction to netrin, we expressed a *clr-1* cDNA under the *mec-7* promoter, which is expressed only in AVM, ALM, PVM, and PLM neurons. *mec-7::clr-1* rescued the effect of the *clr-1* mutation in a *clr-1; slt-1* double mutant, indicating that CLR-1 acts cell-autonomously in AVM to inhibit UNC-40 activity (Fig. 3A). *mec-7::clr-1* did not cause AVM defects by itself (Fig. 3A) or in a *slt-1(eh15)/+* background, indicating that overexpression of *clr-1* did not deregulate its activity.

DCC signaling in AVM is mediated by two downstream signaling pathways, one involving UNC-34, an enabled (Ena) homolog, and the other CED-10, a Rac guanine triphosphatase, and UNC-115, an actin-binding protein similar to human abLIM/limatin (26, 27). To address whether either of these pathways might mediate the CLR-1 effect, we disrupted each branch in a *slt-1* mutant background, where only *unc-40* guidance signaling is active in AVM, and asked whether the *clr-1* mutation could still modify the AVM phenotype. The *clr-1* mutation significantly suppressed the AVM defects of *slt-1; ced-10* and *slt-1; unc-115* but not *slt-1; unc-34* double mutants (Fig. 3B). Thus the *slt-1*;

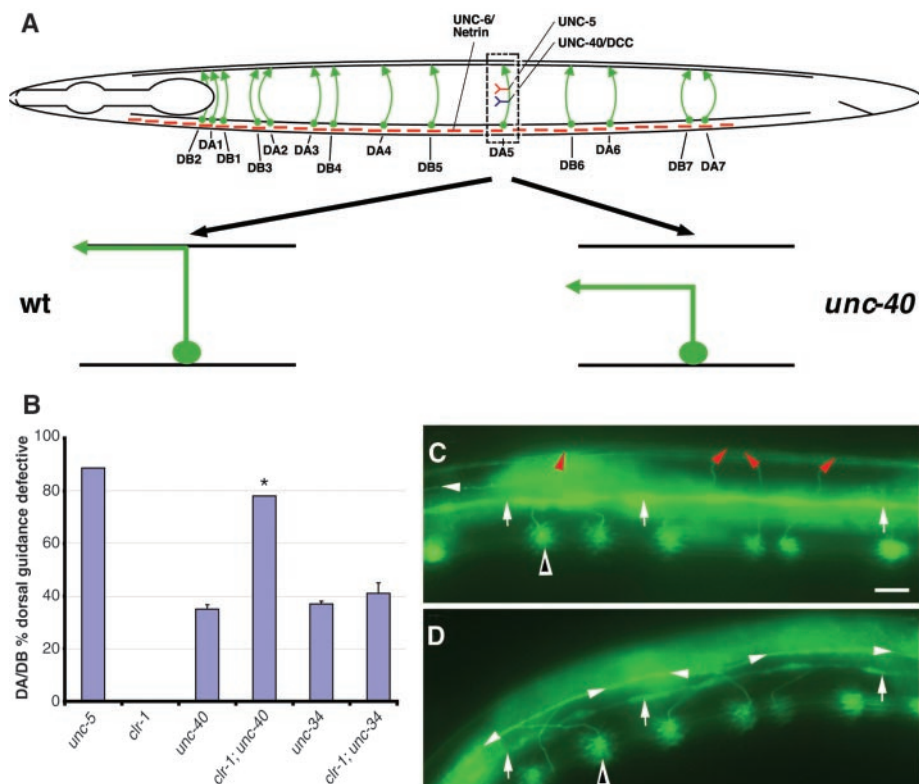


Fig. 2. CLR-1 potentiates UNC-5–dependent repulsion from UNC-6/netrin. (A) Schematic diagram of wild-type (*wt*) and mutant DA/DB motor axon guidance. (B) *clr-1* potentiates DA/DB dorsal guidance. *unc-5* data are from (34). Asterisks, data significantly different from *clr-1*(+) control ($P < 0.001$). DA and DB neurons in L4 stage animals visualized with *evIs82[unc-129::gfp]* in (C) *unc-40* and (D) *clr-1; unc-40*. DA/DB axons in the dorsal nerve cord (red arrowheads) are misrouted to dorsolateral positions (white arrowheads). White arrows indicate lateral seam cells. Open arrowheads, ventral DA/DB cell bodies. Dorsal is up and anterior at left. Scale bar, 20 μ m.

Fig. 3. CLR-1 acts through UNC-34 in AVM. (A) *clr-1* acts cell-autonomously in AVM. Animals expressing *cyEx[mec-7::clr-1, odr-1::dsred]; zds5[mec-4::gfp]* were significantly different from sibling animals that spontaneously lost the *mec-7::clr-1* transgene (asterisk, $P < 0.001$). (B) CLR-1 requires UNC-34 to inhibit UNC-40 signaling. AVM was visualized with *zds5[mec-4::gfp]*. Asterisks indicate data significantly different from *clr-1*(+) controls ($P < 0.001$).

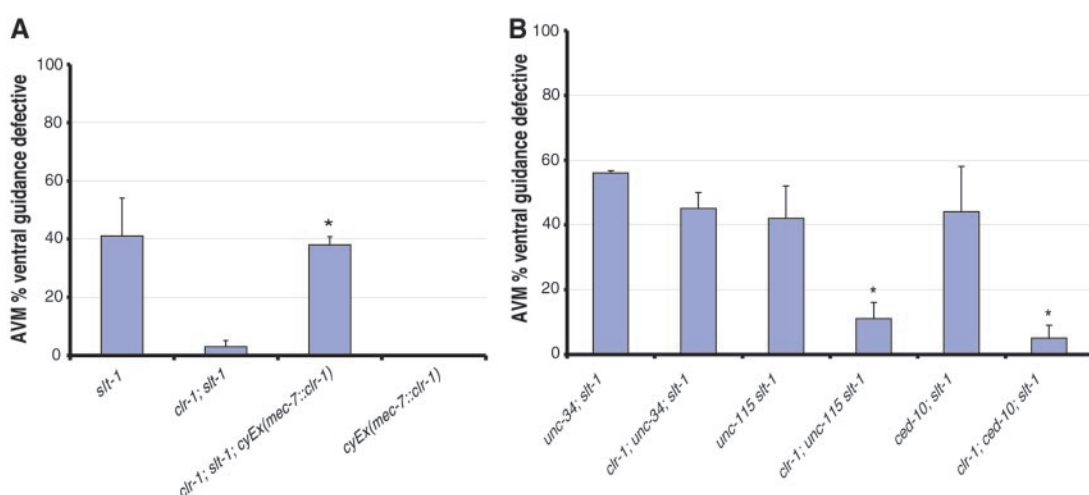
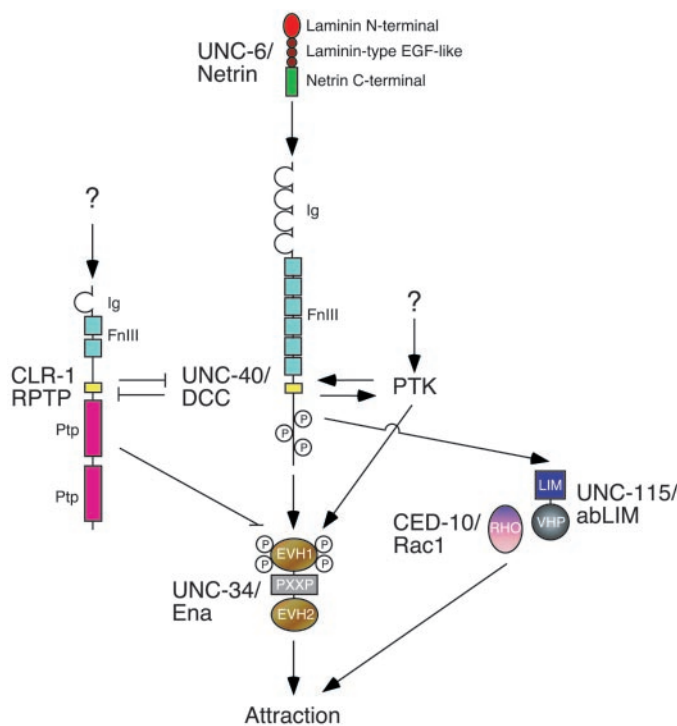


Fig. 4. Model for CLR-1 regulation of netrin attraction. Arrows indicate a positive effect and bars a negative effect. UNC-40, UNC-34, or an unknown effector is phosphorylated by an unknown tyrosine kinase during netrin signaling and dephosphorylated by CLR-1 to inhibit signaling. The cytoplasmic domain of CLR-1 produced in vitro can associate with GS-T:UNC-40 cytoplasmic domain, consistent with a direct interaction of the proteins (33). EGF, epidermal growth factor; PTK, protein tyrosine kinase; PXXP, proline motif. Question marks indicate undefined signaling components.



ced-10 double mutants retain a pathway that is inhibited by CLR-1 and can respond to the mutation, whereas the *slt-1; unc-34* double mutants have lost the CLR-1-sensitive signaling pathway. These results therefore suggest that *clr-1* exerts its negative effect in netrin attraction through the *unc-34*-dependent pathway. In the case of DA and DB axon dorsal guidance, the *clr-1* mutation enhanced *unc-40* mutant phenotypes but not those of *unc-34* mutants (Fig. 2B), indicating that *clr-1* also exerts its positive effect in netrin repulsion through an *unc-34*-dependent pathway. In contrast to its role in attractive and repulsive axon guidance, *clr-1* did not affect an outgrowth-promoting activity of *unc-40* (fig. S3).

Thus, the RPTP CLR-1 functions as a negative regulator of the netrin attractive guidance pathway, acting with or downstream of the netrin receptor UNC-40/DCC in the UNC-34/enabled pathway.

The suppression of ventral guidance defects in *slt-1* mutants by *clr-1* is remarkably complete: Nearly all AVM axons are guided normally in *clr-1; slt-1* double mutants. This result indicates that UNC-6/netrin is sufficient for accurate guidance of AVM even without the dorsal repellent SLT-1, provided the CLR-1 negative regulatory influence is removed. Reducing *clr-1* activity in a wild-

type background did not cause guidance defects, but the null phenotype of *clr-1* is lethal, so only nonnull alleles were examined; stronger axon defects might be observed if *clr-1* function was eliminated. The rate of axon extension is enhanced in neurons from RPTP $\sigma^{-/-}$ mice (28) and in *Xenopus* retinal ganglion cell neurons expressing a dominant negative CRYP (RPTP σ) (29), suggesting a conserved role for RPTPs in inhibiting axon growth.

Our results suggest a model in which a protein tyrosine kinase is a positive regulator of netrin-mediated attraction and CLR-1 is a negative regulator. Such antagonistic effects might reflect opposite effects on the tyrosine phosphorylation state of UNC-40 or of an UNC-40 effector, perhaps UNC-34/enabled (Fig. 4) (30). The enhancement of UNC-40-mediated guidance by removal of CLR-1 identifies a mechanism for negatively regulating netrin attraction and suggests that effects of RPTPs in axon guidance might result from regulation of key axon guidance receptors.

References and Notes

1. M. Tessier-Lavigne, C. S. Goodman, *Science* **274**, 1123 (1996).
2. T. W. Yu, C. I. Bargmann, *Nat. Neurosci.* **4**, 1169 (2001).
3. B. J. Dickson, *Science* **298**, 1959 (2002).

4. H. J. Song, G. L. Ming, M. M. Poo, *Nature* **388**, 275 (1997).
5. K. Hong, M. Nishiyama, J. Henley, M. Tessier-Lavigne, M. M. Poo, *Nature* **403**, 93 (2000).
6. M. Hamelin, Y. Zhou, M. W. Su, I. M. Scot, J. G. Culotti, *Nature* **364**, 327 (1993).
7. K. Hong *et al.*, *Cell* **97**, 927 (1999).
8. K. Keleman, B. J. Dickson, *Neuron* **32**, 605 (2001).
9. E. Stein, M. Tessier-Lavigne, *Science* **291**, 1928 (2001).
10. T. W. Yu, J. C. Hao, W. Lim, M. Tessier-Lavigne, C. I. Bargmann, *Nat. Neurosci.* **5**, 1147 (2002).
11. C. J. Desai, J. G. Gindhart Jr., L. S. Goldstein, K. Zinn, *Cell* **84**, 599 (1996).
12. D. Van Vactor, *Curr. Opin. Cell Biol.* **10**, 174 (1998).
13. U. Drescher *et al.*, *Cell* **82**, 359 (1995).
14. M. Nakamoto *et al.*, *Cell* **86**, 755 (1996).
15. S. McFarlane, E. Cornel, E. Amaya, C. E. Holt, *Neuron* **17**, 245 (1996).
16. F. S. Walsh, P. Doherty, *Annu. Rev. Cell Dev. Biol.* **13**, 425 (1997).
17. F. B. Gertler, R. L. Bennett, M. J. Clark, F. M. Hoffmann, *Cell* **58**, 103 (1989).
18. H. E. Beggs, P. Soriano, P. F. Maness, *J. Cell Biol.* **127**, 825 (1994).
19. W. R. Morse, J. G. Whitesides 3rd, A. S. LaMantia, P. F. Maness, *J. Neurobiol.* **36**, 53 (1998).
20. J. C. Hao *et al.*, *Neuron* **32**, 25 (2001).
21. Information on materials and methods is available on Science Online.
22. M. Kokel, C. Z. Borland, L. DeLong, H. R. Horvitz, M. J. Stern, *Genes Dev.* **12**, 1425 (1998).
23. J. N. Andersen *et al.*, *Mol. Cell Biol.* **21**, 7117 (2001).
24. E. M. Hedgecock, J. G. Culotti, D. H. Hall, *Neuron* **4**, 61 (1990).
25. D. C. Merz, G. Alves, T. Kawano, H. Zheng, J. G. Culotti, *Dev. Biol.* **256**, 173 (2003).
26. Z. Gitai, T. W. Yu, E. A. Lundquist, M. Tessier-Lavigne, C. I. Bargmann, *Neuron* **37**, 53 (2003).
27. E. A. Lundquist, R. K. Herman, J. E. Shaw, C. I. Bargmann, *Neuron* **21**, 385 (1998).
28. K. M. Thompson *et al.*, *Mol. Cell. Neurosci.* **23**, 681 (2003).
29. K. G. Johnson, I. W. McKinnell, A. W. Stoker, C. E. Holt, *J. Neurobiol.* **49**, 99 (2001).
30. The *egl-17* FGF and the *egl-15* FGFR antagonize *clr-1* function in sex myoblast migration (31). *egl-17* null mutations do not affect AVM guidance, whereas *egl-15* mutations partially antagonize *clr-1* (fig. S4). However, this effect could be indirect, because *egl-15* affects axon outgrowth by acting in the epidermis (32) and *egl-15* expression in AVM did not rescue the defect (33).
31. C. Z. Borland, J. L. Schutzman, M. J. Stern, *Bioessays* **23**, 1120 (2001).
32. H. E. Bulow, T. Boulin, O. Hobert, *Neuron* **42**, 367 (2004).
33. C. Chang, C. I. Bargmann, M. Tessier-Lavigne, data not shown.
34. A. Colavita, J. G. Culotti, *Dev. Biol.* **194**, 72 (1998).
35. We thank G. Garriga, S. Clark, and the *Caenorhabditis* Genetics Center for strains; A. Fire for vectors; M. Stern for the *clr-1::GFP* reporter; H. Nguyen for technical support; A. Colavita for critical reading of the manuscript; and members of the Bargmann and Tessier-Lavigne labs for helpful discussions. C.C. is an American Cancer Society Postdoctoral Fellow; T.W.Y. was a MINDS Predoctoral Fellow and a UCSF Medical Scientist Training Program student; and C.I.B. is and M.T.-L. was an Investigator with HHMI.

Supporting Online Material

www.sciencemag.org/cgi/content/full/305/5680/103/DC1
 Materials and Methods
 Figs. S1 to S4
 References

19 February 2004; accepted 1 June 2004

ERRATUM

post date 13 August 2004

REPORTS: "Inhibition of netrin-mediated axon attraction by a receptor protein tyrosine phosphatase" by C. Chang *et al.* (2 July 2004, p. 103). The e-mail address given for the corresponding author, Marc Tessier-Lavigne, is incorrect. The correct e-mail address is marctl@gene.com.